

CONSTRAINTS ON THE COLLISIONAL NATURE OF THE DARK MATTER
FROM GRAVITATIONAL LENSING IN THE CLUSTER A2218PRIYAMVADA NATARAJAN^{1,2}, ABRAHAM LOEB³, JEAN-PAUL KNEIB⁴ & IAN SMAIL⁵¹ Department of Astronomy, Yale University, New Haven, CT, USA² Institute of Astronomy, Madingley Road, Cambridge, CB3 0HA, UK³ Department of Astronomy, Harvard University, 60 Garden Street, Cambridge, MA 02138, USA⁴ Observatoire Midi-Pyrénées, 14 Av. E.Belin, 31400 Toulouse, France⁵ University of Durham, Department of Physics, South Road, Durham DH1 3LE, UK*Draft version February 7, 2020*

ABSTRACT

The detailed distribution of mass within clusters of galaxies can be used to probe the nature of dark matter. We show that constraints on the extent of the mass distribution around galaxies in the rich cluster A 2218 obtained from combining strong and weak lensing observations are consistent with the predictions which assume that the dominant mass component (dark matter) in these halos is collisionless. A strongly interacting (fluid-like) dark matter is ruled-out at a confidence level of more than 5σ .

Subject headings: gravitational lensing, galaxies: fundamental parameters, halos, methods: numerical

1. INTRODUCTION

The detection of gravitational lensing of distant galaxies by foreground galaxies has been used in recent years to set constraints on the masses and sizes of the lensing galaxy halos. Current studies suggest the presence of halos extending beyond 100 kpc (Brainerd, Blandford & Smail 1996; Griffiths et al. 1996; Dell’Antonio & Tyson 1996; Fischer et al. 1999; McKay et al. 2001; Wilson et al. 2001). The same technique can also be applied to galaxies in the dense environments of massive X-ray clusters. Analysis of galaxy-galaxy lensing in the cores of rich clusters implies a smaller spatial extent for the dark matter halos associated with morphologically-classified, early-type cluster members than that seen in the field (Natarajan et al. 1998). Most recently, Natarajan, Kneib, & Smail (2002) [NKS02 hereafter] have found compelling evidence for the tidal truncation of dark matter sub-halos in clusters based on *Hubble Space Telescope* imaging of lensing clusters at intermediate redshifts.

The detailed mass distribution within lensing X-ray clusters, and in particular the fraction of the total cluster mass that is associated with individual galaxies – has important implications for the frequency and nature of galaxy interactions. As we show in this *Letter*, the characteristic halo sizes of cluster galaxies that survive tidal deformation and stripping in their dense environments offer tantalizing clues as to the nature of dark matter itself. While there is incontrovertible evidence for the existence of significant amounts of dark matter in the Universe, its nature remains one of the challenging and unsolved problems in cosmology. Following the original suggestion by Furlanetto & Loeb (2002), we demonstrate here that constraints on the properties of the dark matter, whether it is collisionless or collisional (fluid-like), can be derived based on the truncation radii of galaxy halos in clusters.

If the dark matter is collisionless, then the sizes of galaxy halos in clusters are primarily shaped by the dynamical effects of tidal truncation and collisional stripping (Ghigna et al. 1998). The dominant process of tidal truncation acts

on the short orbital time-scale due to the tidal field of the cluster as a whole (Taylor & Babul 2001), while collisional stripping results from binary interactions among individual galaxies (Binney & Tremaine 1987). The global tidal field of the cluster truncates the dark matter halo of each galaxy at a radius inside of which the mean mass density of the galaxy is roughly equal to the mean interior density of the cluster. However, if the dark matter is fluid-like then galaxy halos would be further stripped by ram pressure down to a radius which is significantly smaller than the tidal radius (roughly by the ratio between the velocity dispersion inside the galaxy halo and the velocity of the galaxy through the cluster; see Furlanetto & Loeb 2002 for further details). In this work, we use the truncation radii of a sample of cluster galaxies, inferred observationally from the galaxy-galaxy lensing in the cluster A 2218 (NKS02), to decide whether the dark matter is collisionless or fluid-like.

2. USING GALAXY-GALAXY LENSING TO MEASURE
TRUNCATION RADII OF CLUSTER GALAXIES

We model the background cluster as a superposition of a smooth large-scale potential ($\sim 250''$ in extent) and small-scale clumps that are associated with bright early-type cluster galaxies (see Natarajan & Kneib 1997 and Natarajan et al. 1998, for more details). To quantify the lensing distortion induced by the global potential, both the smooth component and individual galaxy-scale halos are modeled self-similarly using a surface density profile, $\Sigma(R)$, which is a linear superposition of two pseudo-isothermal elliptical components (see the PIEMD models derived by Kassiola & Kovner 1993),

$$\Sigma(R) = \frac{\Sigma_0 r_0}{1 - r_0/r_t} \left(\frac{1}{\sqrt{r_0^2 + R^2}} - \frac{1}{\sqrt{r_t^2 + R^2}} \right), \quad (1)$$

with a core radius r_0 and a truncation radius $r_t \gg r_0$. The free parameters of this profile are chosen for both the smooth component and the clumps so as to obtain the appropriate mass distributions on the relevant scales. The

projected radius R is a function of the sky coordinates x and y and the ellipticity ϵ (see §2.2 of Natarajan & Kneib 1997). One of the attractive features of this model is that the total mass is finite ($\propto \Sigma_0 r_0 r_t$). With the additional assumption that light traces mass, galaxy halos in clusters are characterized by the following scaling laws:

$$\sigma = \sigma_* \left(\frac{L}{L_*} \right)^{\frac{1}{4}}; r_0 = r_{0*} \left(\frac{L}{L_*} \right)^{\frac{1}{2}}; r_t = r_{t*} \left(\frac{L}{L_*} \right)^{\alpha}. \quad (2)$$

These imply the following scaling for the ratio

$$\frac{r_t}{r_0} = \frac{r_{t*}}{r_{0*}} \left(\frac{L}{L_*} \right)^{\alpha-1/2}. \quad (3)$$

The total mass $M_{\text{tot}}(\infty)$ then scales with the luminosity as

$$M_{\text{tot}}(\infty) = 2\pi \Sigma_0 r_0 r_t = \frac{9\sigma^2}{2G} r_t = \frac{9}{2G} \sigma_*^2 r_{t*} \left(\frac{L}{L_*} \right)^{\alpha+0.5}, \quad (4)$$

and the mass-to-light ratio Υ is given by

$$\Upsilon \sim \left(\frac{\sigma_*}{240 \text{ km s}^{-1}} \right)^2 \left(\frac{r_{t*}}{30 \text{ kpc}} \right) \left(\frac{L}{L_*} \right)^{\alpha-0.5}. \quad (5)$$

For $\alpha = 0.5$ the model has constant Υ for all galaxies (although Υ may be a function of radius inside each galaxy). If $\alpha > 0.5$ ($\alpha < 0.5$) then brighter galaxies have a larger (smaller) Υ than fainter ones. The parameters that characterize both the global smooth component and the clumps are optimized using the observational data (i.e. the positions, magnitudes, geometry of strong lensing features, and the smoothed shear field) as constraints. We find that $\alpha = 0.5$, is the favored value for the best-fit mass models and in fact, $\alpha < 0.5$ is ruled out at a very high confidence.

Our goal is to optimally partition the total cluster mass between a smooth component and the clumps based on the observational data. A maximum-likelihood method is used to obtain significance bounds on fiducial parameters that characterize a typical L_* halo in the cluster. The likelihood function of the estimated probability distribution of the source ellipticities is maximized for a set of model parameters, given a functional form of the intrinsic ellipticity distribution measured for the faint background galaxies. For each faint galaxy j with measured shape τ_{obs} , the intrinsic shape τ_{S_j} can be estimated in the weak regime by subtracting the lensing distortion induced by the smooth cluster and galaxy halos,

$$\tau_{S_j} = \tau_{\text{obs}_j} - \sum_{i=1}^{N_{\text{gal}}} \gamma_{p_i} - \gamma_c, \quad (6)$$

where $\sum_{i=1}^{N_{\text{gal}}} \gamma_{p_i}$ is the sum of the shear contribution at a given position j from N_{gal} galaxies. This entire inversion procedure is performed within the LENSTOOL utilities developed by Kneib (1993), which accurately take into account the non-linearities arising in the strong lensing regime. Using a well-constrained ‘strong lensing’ model for the inner-regions of the cluster along with the averaged shear field and assuming a known functional form for $p(\tau_S)$ from the field, the likelihood for a guessed model is

$$\mathcal{L}(\sigma_*, r_{t*}) = \prod_{j=1}^{N_{\text{gal}}} p(\tau_{S_j}). \quad (7)$$

We compute \mathcal{L} by assigning the median redshift corresponding to the observed source magnitude for each arclight. The best fitting model parameters are then obtained by maximizing the log-likelihood function with respect to the parameters σ_* and r_{t*} . Using a bootstrap method, we have verified that while the convergence to the best-fit model is indeed driven by the brighter cluster galaxies, no single galaxy dominates in the procedure.

3. PROPERTIES OF A 2218

The lens model for the mass distribution in the well-studied cluster A 2218 at $z = 0.17$ is arguably the best constrained case presently available (Kneib et al. 1996), to which we can apply our analysis. We use four sets of multiple images, which are all spectroscopically confirmed at $z = 0.70, 1.03, 2.52$ and 5.60 , in conjunction with the background shear field, to obtain the best-fit parameters for a fiducial L_* galaxy, $r_{t*} = 40^{+30}_{-10}$ kpc and $\sigma_* = 180^{+15}_{-20}$ km s $^{-1}$ (where the quoted error bars are at 5σ confidence). The mass distribution in A 2218 is composed of two clumps centered around the two brightest cluster galaxies, and the profile inferred from lensing observations and X-ray data are consistent. Although the mass distribution is bimodal, we note that the primary clump contributes $\sim 90\%$ of the mass. Nevertheless, we take the presence of the second clump into account when calculating the center-of-mass of the cluster. Below, we tabulate the model parameters for these two components in our best-fit mass model of A 2218.

The morphologies and luminosities of the cluster members (which are crucial for the lensing analysis) are also well-determined from the high-resolution *HST* imaging of this cluster (Smail et al. 2001). We have used the 40 brightest early type-cluster galaxies in the maximum-likelihood analysis to obtain the values quoted above. Their individual truncation radii were then determined by utilizing the scaling laws with luminosity in equation (2). Out of the early-type cluster galaxies selected for the lensing analysis, $\sim 75\%$ are located inside the core-radius and the rest lie interior to 300 kpc, within a few core radii from the cluster center.

There have been several dynamical studies of A 2218 that yielded accurate measurements of galaxy velocities relative to the center of mass of the cluster (Danese, De Zotti & di Tullio 1980; Le Borgne et al. 1992; Girardi et al. 1997; Rakos, Dominis & Steinling 2001). Using the spectro-photometric survey of Le Borgne et al. (1992), we find that 25 of the 40 early-type galaxies in our analysis have measured redshifts which allow us to estimate their velocity relative to the center-of-mass of the cluster. We have then computed the expected truncation radii for these galaxies in two limiting cases regarding the composition of their dark matter halos: (i) collisionless dark matter; and (ii) fluid-like dark matter (see Furlanetto & Loeb 2002).

In our analysis, we have to additionally assume that the orbits of the cluster galaxies under consideration are representative of tidally stripped galaxies. Ghigna et al. (1998) have found that most of the strongly tidally-stripped halos move on nearly radial orbits (since these orbits penetrate the high density core of the cluster) and that radial orbits are overabundant by an order of magnitude relative

Cluster	z	x (arcsec)	y (arcsec)	ϵ	posn. angle (deg)	σ (km s^{-1})	r_0 (kpc)	r_t (kpc)
Main clump	0.17	2.0	0.3	0.3 ± 0.05	-13 ± 5	1070 ± 70	75 ± 10	1100 ± 100
Second clump	0.17	-67.5	3.0	0.2	20 ± 4	400 ± 30	25 ± 5	600 ± 40

to tangential orbits in the inner $r \lesssim 500$ kpc of the cluster. Since we are using the projected location of cluster galaxies in conjunction with their orbital velocities at the present time, the nature of the orbits interior to 300 kpc needs to be established in order to justify the assumption that these galaxies are indeed populating representative orbits for efficient tidal stripping. Using the determined mass profile of the cluster, the line-of-sight velocity dispersion profile and the number density profile of the galaxies, and assuming that cluster galaxies are good tracers of the potential well, we can compute the velocity anisotropy parameter¹, $\beta(r) = (1 - \sigma_t^2/\sigma_r^2)$, via the anisotropic Jeans equation using the approximation of spherical symmetry (for further details see Natarajan & Kneib 1996),

$$\frac{d(\nu_g \sigma_r^2)}{dr} + \frac{2\beta(r)\nu_g \sigma_r^2}{r} = -\frac{G M_{\text{tot}}(r)\nu_g}{r^2}; \quad (8)$$

where $\nu_g(r)$ is three-dimensional galaxy density profile (as derived from the 2D projected distribution via the Abel transform), $\sigma_r^2(r)$ the radial velocity dispersion of the galaxies, and $M_{\text{tot}}(r)$ is the total mass profile. The observed line-of-sight velocity dispersion profile $\sigma_{\text{los}}(R)$ is given by,

$$\frac{1}{2} [\Sigma_g(R) \sigma_{\text{los}}^2(R)] = \int_R^\infty \frac{r \nu_g(r) \sigma_r^2(r) dr}{\sqrt{(r^2 - R^2)}} [1 - \frac{R^2}{r^2} \beta(r)]; \quad (9)$$

The above two integro-differential equations can be solved numerically for σ_r^2 and $\beta(r)$. Substituting the best-fit mass model for A 2218 we obtain $\beta \approx 0.3$, which indicates that the majority of orbits are in fact radial and do plunge through the core of the cluster. Such orbits are likely to facilitate tidal truncation as assumed in our analysis.

4. RESULTS

For collisionless cold dark matter (CDM) the tidal truncation radius, $r_{t,i}$, for the i -th galaxy whose pericenter lies at a radial position r_i inside the cluster, is defined by the condition that the average density of the galaxy halo interior to the tidal radius, matches the mean density of the cluster interior to the galaxy location r_i (Ghigna et al. 1998; Taylor & Babul 2001):

$$\langle \rho_{g_i}(r_{t,i}) \rangle = \langle \rho_{\text{cl}}(r_i) \rangle. \quad (10)$$

For the case of fluid-like dark matter (FDM), the halo truncation process is modified due to the additional process of ram-pressure stripping. In this case the truncation radius is set by the condition (Furlanetto & Loeb 2002),

$$\rho_c(r_i)v_{g_i}^2 = \rho_{g_i}(r_t)\sigma_{g_i}^2, \quad (11)$$

¹Note that $\beta = 0$ implies isotropic orbits, $0 < \beta \leq 1$ implies mostly radial orbits and $\beta < 0$ indicates orbits that are primarily tangential.

²Note that while the truncation radii inferred from the lensing observations are projected 2D values, those calculated from equations (7) and (8) are in 3D. However, because the PIEMD mass density profile is $\rho \propto (r^2 + r_0^2)^{-1}(r^2 + r_t^2)^{-1}$, both truncation radii are equivalent.

where v_{g_i} is the velocity component of the i -th galaxy relative to the cluster center-of-mass, $\rho_{g_i}(r_t)$ is the density of that galaxy halo at its 3D truncation radius r_t , and σ_{g_i} is the internal velocity dispersion of that galaxy². In our analysis, we have conservatively used only the measured component of the velocity of each galaxy (relative to the cluster center) along line-of-sight. Since the full (3D) galaxy velocity can only be larger than our adopted value, our constraint on the truncation radii of galaxies in the FDM case should be regarded as conservative upper limits. The considerations quoted above ignore any further truncation that is likely to be caused by thermal or turbulent heating (Gnedin & Ostriker 2001). Using the above expressions, we derived the truncation radii for the 25 early-type galaxies in A 2218 in the two limiting cases. The results are plotted in Figure 2. The observed distribution of truncation radii from the lensing data analysis (solid triangles) is compared to the radii expected in the collisionless limit (solid squares) and the fluid limit (solid circles). We find that FDM models are ruled-out at a confidence greater than 5σ , while collisionless dark matter models are in excellent agreement with the observationally determined values. We find no correlation between the truncation radii and the orbital velocities for the cluster members in A 2218, as would be expected if ram pressure stripping had been a significant dynamical process in operation.

The association of the retrieved model radius r_{t*} from the lensing analysis with the tidally truncated radius is strengthened through the following observed correlation. For a galaxy described by a PIEMD mass profile with velocity dispersion $\sigma_{0,i}$ and whose orbital pericenter crosses the cluster core where the density is ρ_0 , the tidal truncation radius scales as

$$r_t \propto \sigma_{0,i} \rho_0^{-\frac{1}{2}}. \quad (12)$$

Deriving the best-fit values of ρ_0 from the strong lensing models and $\sigma_{0,i}$ from the maximum-likelihood analysis, we find that the above simple scaling adequately reproduces the observed trends both for the truncation radius and the mass of a fiducial halo in the five *HST* clusters studied in NKS02 (ranging in redshift from $z = 0.17$ – 0.58). The trends seen in halo size r_t^* with redshift from the lensing study of NKS02 are also in good agreement with the theoretical expectation from numerical simulations (Ghigna et al. 1998). High resolution collisionless N-body simulations of cluster formation and evolution, predict that the dominant interaction is between the global cluster tidal field and individual galaxies in the redshift interval $z \sim 0$ – 0.5 (Ghigna et al. 1998; Moore et al. 1996).

5. CONCLUSIONS AND DISCUSSION

We have used gravitational lensing data to constrain the truncation radii of galactic dark matter halos in the cluster A 2218. Figure 2 shows that the inferred truncation radii are consistent with the tidal radii expected for collisionless dark matter, but rule-out fluid-like dark matter for which ram pressure stripping is effective.

The transition between the collisionless and collisional regimes is set by the ratio between the mean-free-path of dark matter particles, λ , and the radius, r_t , of the galaxy halos under consideration. This ratio is given by,

$$\frac{\lambda}{r_t} \approx \frac{m_p}{\sigma_p \Sigma(r_t)}, \quad (13)$$

where σ_p/m_p is the collisional cross-section per unit particle mass and $\Sigma(r_t)$ is the surface mass density of a galaxy halo at its truncation radius. The fluid regime is obtained for $\frac{\lambda}{r_t} \lesssim 1$. The characteristic surface mass densities of the galaxies in A 2218 can be directly inferred from the analysis of the lensing data. We find that for an L_\star galaxy, $\Sigma_\star(r_t) \approx 0.024 \text{ g cm}^{-2}$. Since the fluid regime is ruled out, we exclude all values of $\sigma_p/m_p \gtrsim 42 \text{ cm}^2 \text{ g}^{-1}$.

Our constraints are complementary to those derived by

Gnedin & Ostriker (2001) from considerations of thermal conduction in the mildly collisional regime. These authors exclude the regime $0.3 \lesssim \sigma_p/m_p \lesssim 10^4 \text{ cm}^2 \text{ g}^{-1}$, based on the consideration that cluster ellipticals will otherwise deviate from the fundamental plane beyond the observed scatter. Our new constraint allows us to rule out the high cross-section regime and hence we conclude that $\sigma_p/m_p \lesssim 0.3 \text{ cm}^2 \text{ g}^{-1}$ as an absolute upper limit. Dark matter cross-sections higher than this upper limit were postulated by Spergel & Steinhardt (2000) in order to reconcile problems that cold dark matter models possess when compared to observational data (such as the abundance of galactic sub-halos and the slope of the inner mass density profile of galaxies; see further discussion in Dave et al. 2001; Yoshida et al. 2000; Stoehr et al. 2002; Miralda-Escude 2002).

PN acknowledges support from a Trinity College Research Fellowship. This work was supported in part by NSF grants AST-9900877, AST-0071019 for AL. JPK thanks the CNRS and the TMR-Lensing collaboration and IRS the Royal Society and the Leverhulme Trust for support.

REFERENCES

Binney, J., & Tremaine, S., 1987, Galactic Dynamics, (Princeton: Princeton U. Press), Ch. 7

Brainerd, T., Blandford, R., & Smail, I., 1996, ApJ, 466, 623

Couch, W.J., Barger, A.J., Smail, I., Ellis, R.S., Sharples, R.M., 1998, ApJ, 497, 188

Danese, L., de Zotti, G., & di Tullio, G. 1980, ApJ, 82, 322

Dave, R., Spergel, D., Steinhardt, P. J., & Wandelt, B. 2001, ApJ, 547, 574

Dell' Antonio, I., & Tyson, J. A. 1996, ApJ, 473, L17.

Fischer, P., et al. 2000, AJ, 120, 1198

Furlanetto, S., & Loeb, A. 2002, ApJ, 565, 854

Ghigna, S., Moore, B., Governato, F., Lake, G., Quinn, T., & Stadel, J. 1998, MNRAS, 300, 146

Girardi, M., et al. 1997, ApJ, 490, 56

Gnedin, O., & Ostriker, J. P. 2001, ApJ, 561, 61

Griffiths, R. E., Casertano, S., Om, M., & Ratnatunga, K. U. 1996, MNRAS, 282, 1159

Kassiola, A., & Kovner, I. 1993, ApJ, 417, 474

Kneib, J-P., Ellis, R. S., Couch, W., Smail, I. R., & Sharples, R. 1996, 471, 643

Le Borgne, J-F., Pello, R., & Sanahuja, B. 1992, A&AS, 95, 87

McKay, T. et al. 2002, ApJ, submitted (astro-ph/0108013)

Miralda-Escude, J. 2002, ApJ, 564, 1019

Moore, B., Katz, N., Lake, G., Dressler, A., & Oemler, A. 1996, Nature, 379, 613

Natarajan, P., & Kneib, J-P. 1996, MNRAS, 283, 1031

Natarajan, P., & Kneib, J-P. 1997, MNRAS, 287, 833

Natarajan, P., Kneib, J-P., Smail, I., & Ellis, R. S. 1998, ApJ, 499, 600

Natarajan, P., Kneib, J-P., & Smail, I. 2002, ApJ, submitted

Rakos, K., Dominis, D., & Steindling, S. 2000, A&A, 369, 750

Smail, I., et al. 1997, ApJS, 110, 213

Smail, I., et al. 2001, MNRAS, 323, 839

Spergel, D., & Steinhardt, P. J. 2000, Phys. Rev. Lett., 84, 17, 3760

Stoehr, F., et al. 2002, preprint, astro-ph/0203342

Taylor, J. E., & Babul, A. 2001, ApJ, 559, 716

Yoshida, N., Springel, V., White, S. D. M., & Tormen, G. 2000, ApJ, 535, L103

Wilson, G., Kaiser, N., Luppino, G. A., & Cowie, L. L. 2001, ApJ, 555, 572

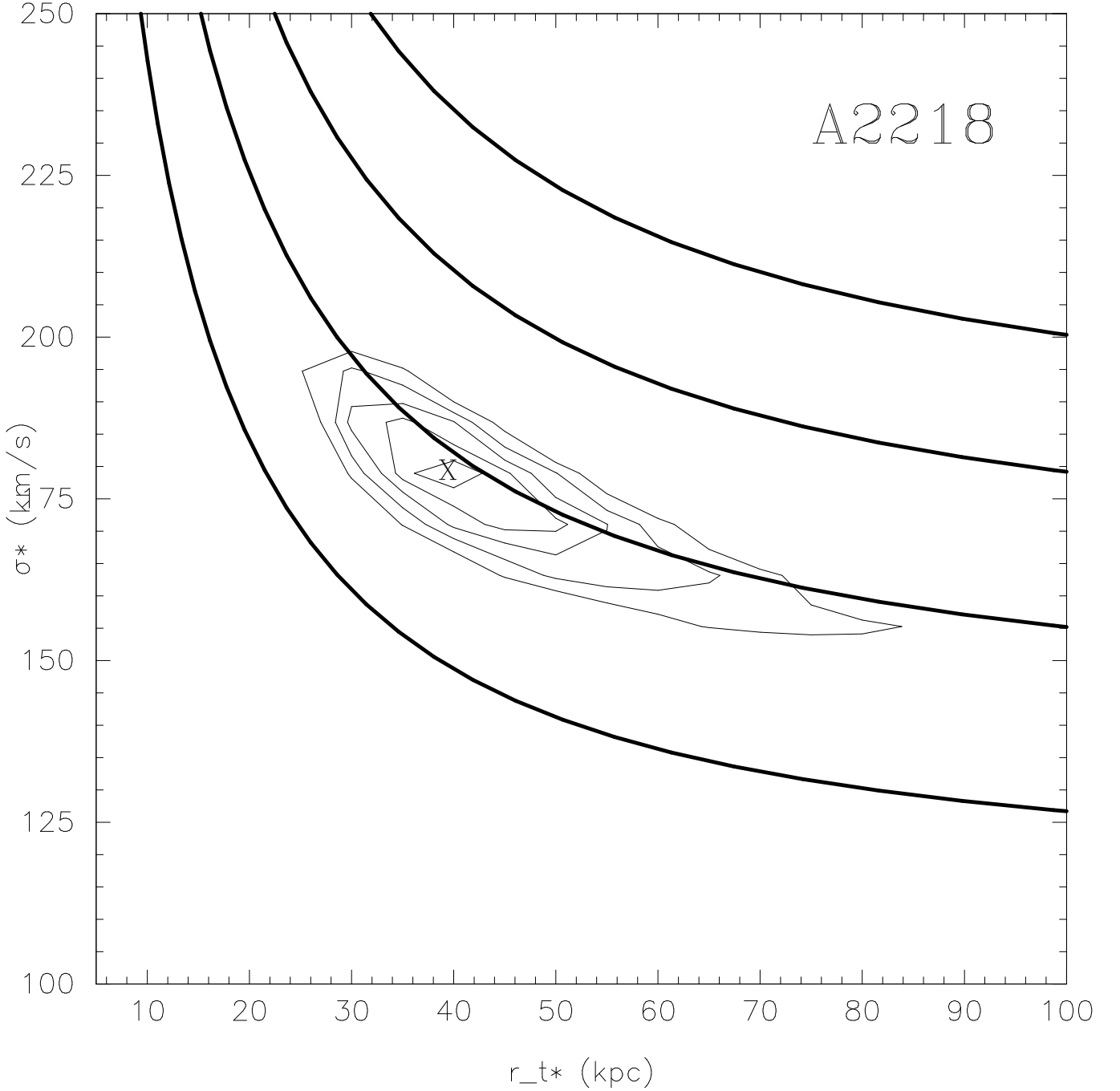


FIG. 1.— Results of maximum-likelihood analysis of lensing data for the cluster A 2218 (NKS02). The contour plot shows the best-fit values for the model parameters σ_* and r_{t*} , which are the central velocity dispersion and truncation radius for a typical L_* galaxy in the cluster. The likelihood contours are plotted in intervals of $1 - \sigma$ starting from the inside out. The thick open curves are lines of constant enclosed mass.

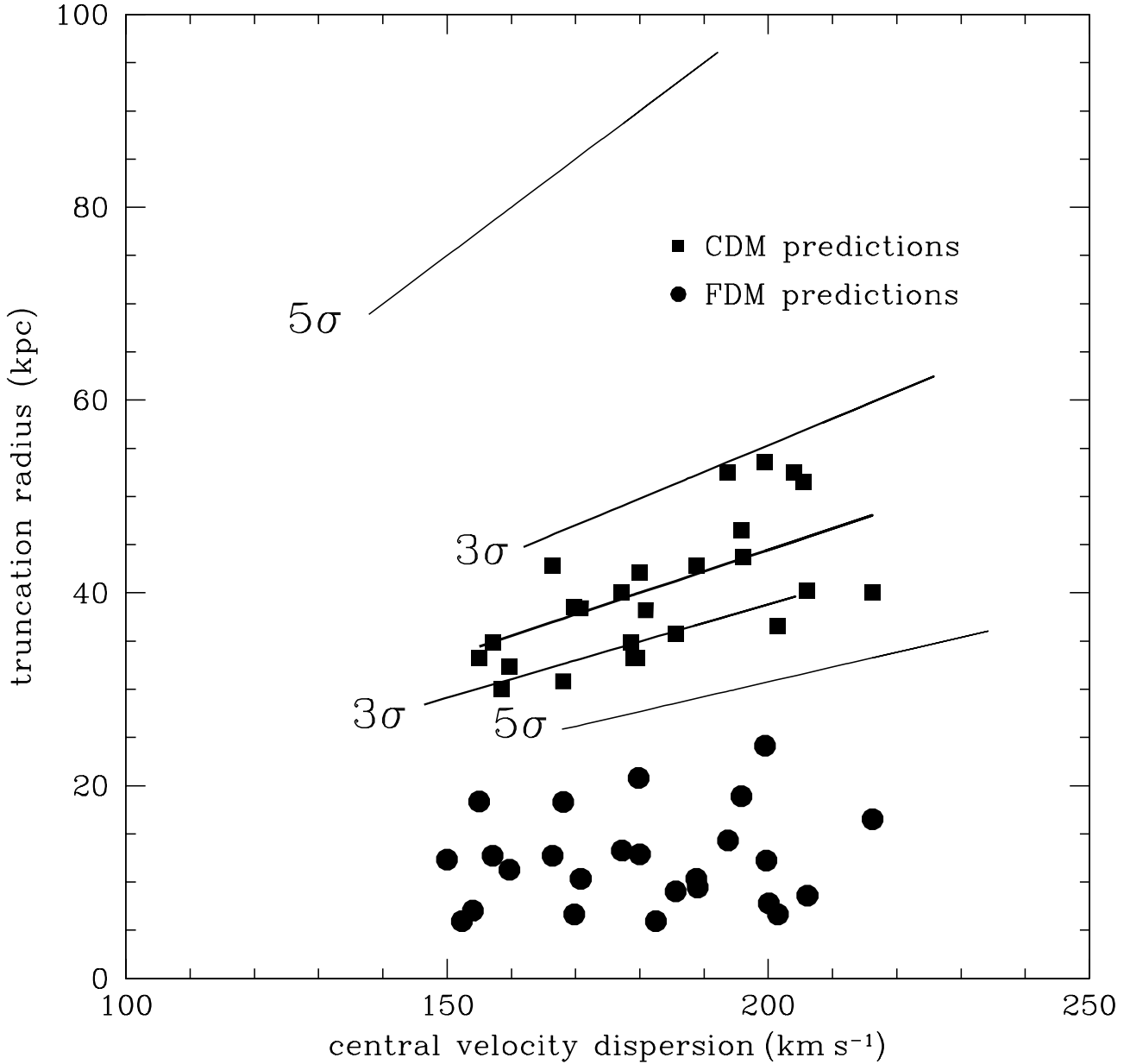


FIG. 2.— Distribution of truncation radii as inferred from the lensing analysis of 25 galaxies superimposed on the scaling relation (thick solid line) in the cluster A 2218. The 3- σ and 5- σ lines denote the corresponding confidence levels in the parameters r_{t*} , and σ^* obtained for a typical L_* galaxy in this cluster (derived from the confidence level contours in Figure 1). The expected distribution of tidal radii for fluid-like dark matter (FDM; solid circles) and collisionless cold dark matter (CDM; solid squares) are also shown. Note that the linear relation between truncation radius and velocity dispersion for the values inferred from lensing is a consequence of the assumed scaling laws with galaxy luminosity [equation (2)].